Journal of Inorganic Biochemistry 193 (2019) 143–151

Contents lists available at ScienceDirect

Journal of Inorganic Biochemistry

journal homepage: www.elsevier.com/locate/jinorgbio

Lycopene attenuates aluminum-induced hippocampal lesions by inhibiting oxidative stress-mediated inflammation and apoptosis in the rat

Zheng Cao[a,b], Peiyan Wang[a], Xiang Gao[a,b], Bing Shao[a,b], Shuchen Zhao[a,*], Yanfei Li[a,*]

[a] College of Veterinary Medicine, Northeast Agricultural University, Harbin 150030, China
[b] Northeastern Science Inspection Station, China Ministry of Agriculture Key Laboratory of Animal Pathogen Biology, Northeast Agricultural University, Harbin 150030, China

ARTICLE INFO

Keywords:
Aluminum chloride ; lycopene ; hippocampal lesions ; Nrf2 ; inflammation ; apoptosis

ABSTRACT

Aluminum (Al) causes hippocampal lesions by oxidative stress, which is widely accepted as the primary pathogenesis of Al neurotoxicity. Lycopene (LYC), a naturally carotenoid, has received extensive attention due to its antioxidant effect. In this study, the neuroprotective effects and mechanisms of LYC against aluminum chloride ($AlCl_3$)-induced hippocampal lesions were explored. First, oral administration of LYC (4 mg/kg) alleviated $AlCl_3$-induced (150 mg/kg) cognition impairment and histopathological changes of the hippocampus in rats. Then, LYC significantly attenuated $AlCl_3$-induced oxidative stress, presenting as the reduced reactive oxygen species, malondialdehyde and 8-hydroxy-2′-deoxyguanosine levels, and increased glutathione level and superoxide dismutase activity. Moreover, LYC also protected the hippocampus from $AlCl_3$-induced apoptosis and neuroinflammation, as assessed by protein levels of p53, Bcl-2-associated X protein (Bax), B-cell lymphoma gene 2 (Bcl-2), Cytochrome c (Cyt c), cleaved caspase-3 and nuclear factor kappa B, as well as the mRNA levels of Bax, Bcl-2, tumor necrosis factor alpha, interleukin-6 and interleukin-1 beta. Finally, LYC increased nuclear factor-erythroid-2-related factor 2 (Nrf2) nuclear translocation and its downstream gene expression, including heme oxygenase-1, NAD(P)H: quinone oxidoreductase 1, glutamate cysteine ligase catalytic subunit and superoxide dismutase 1, which were involved in antioxidant, anti-apoptosis, and anti-inflammation. Overall, our findings demonstrate LYC attenuates Al-induced hippocampal lesions by inhibiting oxidative stress-mediated inflammation and apoptosis in the rat.

1. Introduction

Aluminum (Al), an accumulative neurotoxic metal, causes learning and memory ability impairments in humans and animals [1,2]. Although the neurotoxicity of Al is a well-established fact in mammals now, Al remains widely used in daily life, such as water purifiers, food additives and pharmaceuticals [3–5]. Moreover, acid rain and bauxite mines exploitation can result in the discharge of Al salts from insoluble minerals, raising the risk of human contact with Al [6,7]. Al can penetrate the blood-brain barrier and accumulate in all brain regions [8]. Hippocampus, the site of memory and learning, is the brain regions of Al maximum accumulation after Al intoxication [9]. Al induces imbalance between cellular reactive oxygen species (ROS) production and antioxidant capacity in the hippocampus, and thereby causes oxidative stress and apoptotic cell death, resulting in hippocampal lesions [10–12]. Furthermore, recent studies showed ROS activates nuclear factor κB (NF-κB) and increases inflammatory mediators, such as inducible tumor necrosis factor α (TNF-α), Interleukin-6 (IL-6) and Interleukin-1β (IL-1β), subsequently causes secondary neuronal insult [13–15]. Therefore, antioxidant was considered as a potential therapeutic or preventive strategies of Al-induced hippocampal lesions.

The nervous system has neuroprotective mechanism against oxidative stress. The nuclear factor-erythroid-2-related factor 2 (Nrf2), a regulator of redox homeostasis, can enhance antioxidant defense capability by increasing the expression of antioxidant genes to protect the nervous system [16]. A recent study showed that the mechanism of Al neurotoxicity is associated with dysregulation of Nrf2 signaling [17]. Moreover, sulforaphane, an activator of Nrf2, protects the hippocampus against Al-induced learning and memory deficits [18]. Therefore, Nrf2 activation may have the potential therapeutic or preventive effect in Al-induced neurotoxicity.

Lycopene (LYC) is a naturally occurring carotenoid found in

* Corresponding authors at: College of Veterinary Medicine, Northeast Agricultural University, NO. 600 Changjiang Street, Xiangfang District, Harbin 150030, China.
E-mail addresses: zscrichard@163.com (S. Zhao), liyanfei@neau.edu.cn (Y. Li).

https://doi.org/10.1016/j.jinorgbio.2019.01.017
Received 26 June 2018; Received in revised form 28 January 2019; Accepted 31 January 2019
Available online 01 February 2019
0162-0134/

tomatoes and other red fruit, such as watermelons, papayas and guava [19]. LYC has received rapidly soaring attention due to its various health-beneficial bioactivities such as antioxidant defense, anticancer and cardiovascular protective effects with few side effects [20–22]. In addition, recent studies showed LYC possesses potential neuroprotective effects against amyloid β protein, lipopolysaccharide and D-galactose-induced neurological disorders by antioxidant, anti-inflammatory and anti-apoptosis [23–25]. Nevertheless, it remains unknown about the protective role of LYC against Al-induced neurotoxicity. Therefore, this study was aimed to investigate the possible protective effect of LYC on Al-induced hippocampal lesions and explore its detailed mechanisms.

2. Materials and methods

2.1. Animals and treatment

Seventy-two male Wistar rats (three-weeks old) were purchased from the Experimental animal center of Harbin Medical University (Harbin, China). The rats were housed under standard conditions according to a previous method [2]. After five days of acclimatization, the rats were randomly divided into four groups ($n = 18$ per group). Group 1 (Control) was administered with vehicle by oral gavage. Group 2 (Al) was administered with $AlCl_3$ at 150 mg/kg/day and vehicle of LYC by oral gavage. Group 3 (Al + LYC) was administered with $AlCl_3$ at 150 mg/kg/day and LYC at 4 mg/kg/day by oral gavage. Group 4 (LYC) was administered with vehicle of $AlCl_3$ and LYC at 4 mg/kg/day by oral gavage. $AlCl_3$ (Aladdin, Shanghai, China) was dissolved in distilled water, and then administered according to the values of oral uptake promoted neurotoxicity on rats [2]. LYC (≥ 96%, Jingzhu, Nanjing, China) was dissolved in distilled water with 5% Tween 80, and then administered according to values of oral uptake promoted neuroprotective on rats [26]. The rats were daily administered with $AlCl_3$ 12 h prior to LYC administration for 90 days. To maintain a constant $AlCl_3$ and LYC intake, we measured the body weight every five days and then adjusted the dose accordingly. The animal procedures were approved by the Animal Ethics Committee of the Northeast Agricultural University (Harbin, China).

2.2. Morris water maze

Six rats were randomly selected from each group for the Morris water maze (MWM) test. MWM was performed same as described previously [2]. Briefly, to assess spatial learning, the rats went through an acquisition trial on 1–5 days, then on day 6 probe trial to assess spatial memory. The MWM (Xinruan Information Technology, Shanghai, China) was a black circular pool (160 cm in diameter, 50 cm high) filled with water (30 cm in depth) at 22 ± 1 °C. In the acquisition trial, a transparent round platform was placed below the water surface of northeast quadrant in a circular pool. The rats were placed for 30 s on the platform, and then were placed at a starting point in the middle of the rim of a quadrant with them facing to the wall. The rats swam freely until they reached the platform. The rats that failed to reach the platform within 90 s were guided to the platform and allowed to stay on it for 30 s. We trained the rats for 5 days with three trials per day (8:00 a.m–12:00 p.m) at 10 mins interval. In the probe trial, the escape platform was removed. The rats were placed gently at the start point of southwest quadrant and allowed to swim freely for 90 s. We recorded the number of crossings platform location and the time that the rats spent swimming in target quadrant.

2.3. Tissue sample preparation

The rats were sacrificed after anesthesia (50 mg/kg, sodium pentobarbital, i.p.). We chose the rats that were exposed to the MWM for hematoxylin and eosin (HE) staining and measurement hippocampal Al level. The half of the brain fixed in 10% formalin for HE staining, and the hippocampus of the other half of the brain (frozen rapidly in liquid nitrogen and then stored at −80 °C) was used for measurement hippocampal Al level. We chose the other rats that were not exposed to the MWM for subsequent study. The hippocampus was excised immediately and washed in ice-cold saline. Part was used to prepare hippocampus homogenate for assay of oxidative stress markers, and a portion (frozen rapidly in liquid nitrogen and then stored at −80 °C) was used for hippocampus RNA and protein extraction. The body weight and hippocampal weight ($n = 12$ per group) was measured. The hippocampal coefficients were calculated by multiplying the hippocampal weight (g)/body weight (g) with 100%.

2.4. Histopathological analysis

The brain ($n = 6$ per group) was fixed with 10% neutral buffered formalin for 72 h, and processed using routine histological techniques. After paraffin embedding, 5 μm sections were cut and stained with HE staining to assess tissue structure according to the previous study [27]. The slides were visualized using light microscopy (Nikon, Japan). The extent of the neuronal damage was quantifed by counting the number of normal pyramidal neurons (without any pathological alteration) in the CA1 and CA3 region of the hippocampus, which was expressed as the number of neurons per unit length (mm).

2.5. Measurement of hippocampal Al level

We determined the hippocampal Al level with graphite furnace atomic absorption spectrophotometry as described previously [28]. 0.05 g hippocampus was dried in a dryer (80 °C) for 12 h. We added the dried tissue to a triangle flask, added 10 ml nitric acid and perchloric acid mixture (volume ratio is 4:1), mixed and overnight. Then the mixture were heated slowly on an electric stove till it became colorless and transparent. After cooling it well, the mixture were diluted to 10 ml with 0.5% nitric acid. The Al standard solution was made by mixing 1 ml Al standard reserve liquid (1000 μg/ml, Shines East Chemical Co., Ltd., Guangzhou, China) and 99 ml deionized water. The absorbency was determined by a PEAA800 atomic absorption spectrophotometer (Perkin Elmer, Fremont, CA, USA) using a wavelength of 309.3 nm, slit width of 0.7 nm, lamp current of 15.0 mA, and an injection volume of 20 μl. We examined each sample ($n = 6$ per group) in triplicate and calculated a mean value.

2.6. Measurement of oxidative stress markers

The ROS level, malondialdehyde (MDA) level, glutathione (GSH) level, superoxide dismutase (SOD) activity and 8-hydroxy-2′-deoxyguanosine (8-OHdG) level in the hippocampus was detected by commercially available kits (Nanjing Jiancheng Bioengineering Institute, Nanjing, China). Briefly, the assay of ROS was determined using 20, 70-dichlorofluorescin diacetate (DACHA). The fluorescence was determined at 488 nm excitation and 525 nm emission wavelength, using a fluorescence spectrophotometer (Infinite M200 PRO Tecan, Switzerland). The MDA levels, GSH levels and SOD activity were measured according to the manufacturer's instructions. The absorbance was measured using a spectrophotometer (Spectrum Instruments Co., Ltd., Shanghai, China) at 532 nm, 405 nm and 450 nm, respectively. The 8-OHdG levels were measured by Rat 8-OHdG ELISA Assay Kit. The optical density was measured using a 318 MC microplate reader (Shanghai Sanco Instrument Co., Ltd., Shanghai, China) at 450 nm. We examined each sample ($n = 6$ per group) in triplicate and calculated a mean value.

2.7. Quantitative real-time PCR

The mRNA levels of Bcl-2-associated X protein (Bax), B-cell

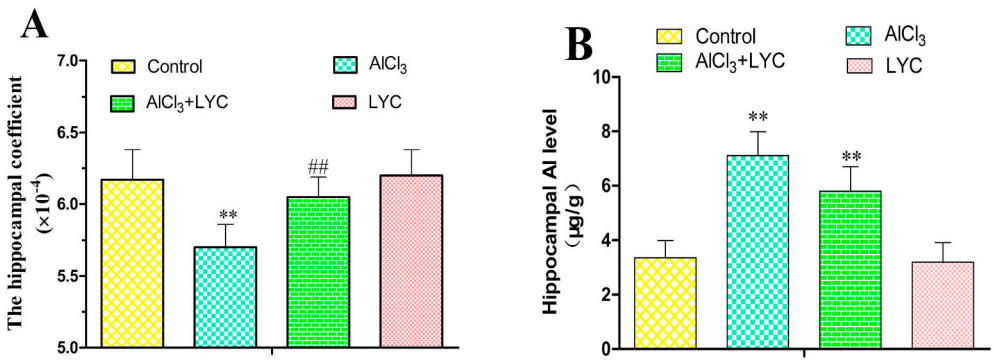

Fig. 1. Effects of LYC on hippocampal coefficient and hippocampal Al level in $AlCl_3$-exposed rats. (A) The hippocampal coefficient. (B) Hippocampal Al level.

lymphoma gene 2 (Bcl-2), IL-1β, TNF-α, IL-6, heme oxygenase-1 (HO-1), NAD(P)H: quinone oxidoreductase 1 (NQO1), glutamate cysteine ligase catalytic subunit (GCLC) and superoxide dismutase 1 (SOD1) were detected by quantitative real-time reverse transcription-polymerase chain reaction as described previously [29]. Total RNA was extracted from the hippocampus using Trizol Reagent (Invitrogen, Waltham, USA) according to the manufacturer's instructions, and then reversely transcribed each sample into cDNA using Trans Script First-Strand cDNA Synthesis Super Mix (Trans Gen Blotech, Beijing, China). We used SYBR Green/Fluorescence in qPCR Master Mix and the ABI PRISM 7500 Real-Time PCR System (Applied Biosystems, Waltham, USA) to examine gene expression. We used β-actin mRNA as internal control to adjust the amount of mRNA in each sample. We examined each sample ($n = 6$ per group) in triplicate and calculated a mean value. The primer sequences that we used for this study are as shown Supplementary Table 1.

2.8. Western blot

Cytoplasmic and nuclear proteins were extracted from the hippocampus using Nuclear and Cytoplasmic Protein Extraction kit (Beyotime Biotechnology, Nantong, China). For Western blot, as described previously [27], the protein was separated in 12% sodium dodecylsulfate-polyacry-lamide gel electrophoresis and transferred to polyvinylidene difluoride membrane (Millipore, Bedford, USA). The membranes was blocked with 5% fat-free milk in Tris buffered saline Tween at 37 °C for 3 h, and then incubated with anti-Nrf2 (Wanlei Biotechnology, Shenyang, China), anti-NF-κB p65 (Bioss Biotechnology, Beijing, China), anti-p53 (Wanlei Biotechnology, Shenyang, China), anti-Cytochrome c (cyt c) (Santa Cruz Biotechnology, Texas, USA), anti-B-cell lymphoma gene 2 (Bcl-2) (Wanlei Biotechnology, Shenyang, China), anti-Bcl-2-associated X protein (Bax) (Wanlei Biotechnology, Shenyang, China), anti-cleaved caspase-3 (Wanlei Biotechnology, Shenyang, China), anti-β-actin (Wanlei Biotechnology, Shenyang China) and anti-Lamin B1 (Boster Biotechnology, Wuhan, China.) in 5% fat-free milk overnight at 4 °C overnight. Subsequently, the primary antibodies were localized with goat anti-rabbit IgG (H + L) and goat anti-mouse IgG (H + L) (Beytime Biotechnology, Nantong, China) for 2 h at 37 °C. Then protein level was determined using the enhanced chemiluminescent reagent (Beytime Biotechnology, Nantong, China). The densitometric measurements were determined using the Image-J software. We examined each sample ($n = 6$ per group) in triplicate and calculated a mean value.

2.9. Statistical analysis

Data are expressed as mean ± standard deviation (SD). The results were analyzed by One-way analysis of variance followed by Bonferroni's test (SPSS 22.0 software; SPSS Inc., Chicago, IL, USA). We considered p-values of < 0.05 as significant and < 0.01 as markedly significant.

3. Results

3.1. Effects of LYC on body weight, hippocampal coefficient and hippocampal Al level in $AlCl_3$-exposed rats

For the body weights, there were no significant differences ($p > 0.05$) among the groups (Supplementary Fig. 1). The hippocampal coefficient in the $AlCl_3$ group was lower ($p < 0.01$) than that in the control group, and hippocampal coefficient in the $AlCl_3$ + LYC group was higher ($p < 0.01$) than that in the $AlCl_3$ group (Fig. 1A). The hippocampal Al level of $AlCl_3$ group and $AlCl_3$ + LYC was higher ($p < 0.01$) than that of control group, and the hippocampal Al level of $AlCl_3$ + LYC group was lower than that of $AlCl_3$ group, but it was not statistically significant ($p > 0.05$) (Fig. 1B).

3.2. Effects of LYC on learning and memory in $AlCl_3$-exposed rats

In acquisition trial, the escape latency of the $AlCl_3$ + LYC group and the LYC group was not different ($p > 0.05$) as compared to that of the control group in five days, but escape latency of the $AlCl_3$ group was longer ($p < 0.05$) than that of the control group from the third to fifth days. The escape latency of the $AlCl_3$ + LYC group was shorter ($p < 0.05$) than that of the $AlCl_3$ group in fourth and fifth days (Fig. 2A). In probe trial, the time spent in target quadrant by the $AlCl_3$ + LYC group and the LYC group was similar ($p > 0.05$) to that of the control group, but the time spent by the $AlCl_3$ group in the target quadrant was shorter ($p < 0.01$) than that by the control group. The time spent by the $AlCl_3$ + LYC group in the target quadrant was longer ($p < 0.05$) than that by the $AlCl_3$ group (Fig. 2B). Additionally, the number of crossings platform position in the $AlCl_3$ + LYC group and the LYC group was not different ($p > 0.05$) as compared to that in the control group, but the number of crossings platform position in the $AlCl_3$ group was less ($p < 0.01$) than that in the control group. The number of crossings platform position in the $AlCl_3$ + LYC group was more ($p < 0.05$) than that in the $AlCl_3$ group (Fig. 2C). These results indicate LYC administration improves learning and memory in $AlCl_3$-exposed rats.

3.3. Effects of LYC on the histopathology of hippocampus in $AlCl_3$-exposed rats

The micrographs of HE staining (Fig. 3) showed that the CA1 and CA3 regions of the hippocampal neurons presented regular arrangement, clear nucleus and nucleolus without any pathological alteration in the control group and the LYC group. In the $AlCl_3$ group, the hippocampal neurons presented irregular arrangement, enlarged

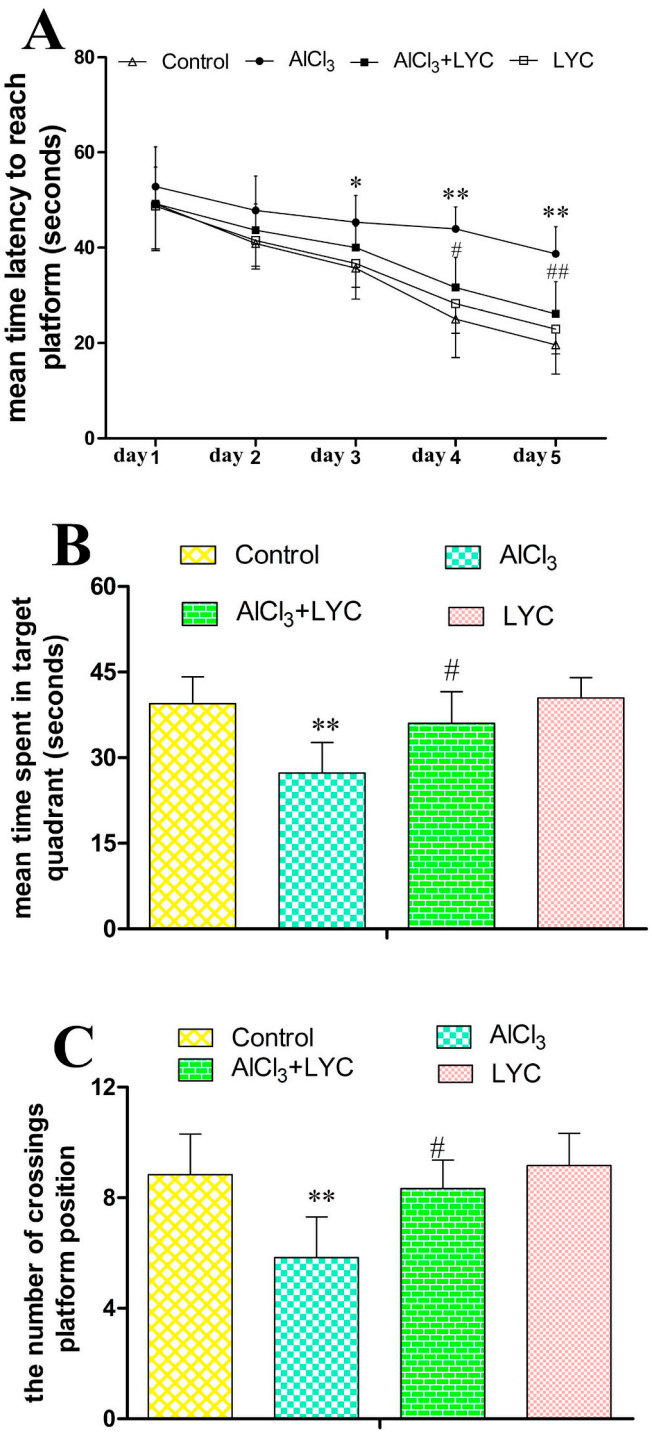

Fig. 2. Effects of LYC on hippocampal-dependent learning and memory ability in $AlCl_3$-exposed rats. Acquisition trials: (A) mean time to reach platform. Probe trials: (B) mean time spent in target quadrant and (C) the number of crossings platform location.

pericellular space, unclear nuclear structure, pyknotic nuclei and necrosis. While, the hippocampal neurons of the $AlCl_3$ + LYC group showed a relatively normal morphological appearance of the nerve cells with few enlarged pericellular space and necrosis. Additionally, the number of normal pyramidal neurons in the $AlCl_3$ group was lower ($p < 0.01$) than that in the control group, and the number of normal pyramidal neurons in the $AlCl_3$ + LYC group was higher ($p < 0.05$) than that in the $AlCl_3$ group. These results indicate LYC administration attenuates $AlCl_3$-induced hippocampal lesions in rats.

3.4. Effects of LYC on oxidative stress in the hippocampus of $AlCl_3$-exposed rats

As shown in Fig. 4, the levels of ROS, 8-OHdG and MDA in the $AlCl_3$ group were higher ($p < 0.01$) than these in the control group, and the levels of ROS, 8-OHdG and MDA in the $AlCl_3$ + LYC group were lower ($p < 0.01$) than these in the $AlCl_3$ group. Additionally, the SOD activity and GSH level in the $AlCl_3$ group was lower ($p < 0.01$) than that in the control group, and the SOD activity and GSH level in the $AlCl_3$ + LYC group was higher ($p < 0.05$) than that in the $AlCl_3$ group.

3.5. Effects of LYC on apoptosis in the hippocampus of $AlCl_3$-exposed rats

As shown in Fig. 5, the protein levels of p53, cytoplasmic Cyt c and cleaved caspase-3 in the $AlCl_3$ group were higher ($p < 0.01$) than these in the control group. In addition, the protein and mRNA level of Bax in the $AlCl_3$ group was higher ($p < 0.01$) than that in the control group, the protein and mRNA level of Blc-2 in the $AlCl_3$ group was lower ($p < 0.01$) than that in the control group. However, compared with the group only receiving $AlCl_3$, LYC significantly reversed these effects ($p < 0.01$).

3.6. Effects of LYC on neuroinflammation in the hippocampus of $AlCl_3$-exposed rats

As shown in Fig. 6, the mRNA levels of IL-1β, TNF-α and IL-6 in the $AlCl_3$ group were higher ($p < 0.01$) than these in the control group, and the mRNA levels of IL-1β, TNF-α and IL-6 in the $AlCl_3$ + LYC group were lower than these in the $AlCl_3$ group ($p < 0.01$). These results suggest that LYC administration attenuates $AlCl_3$ induced inflammation in the hippocampus. Additionally, the nuclear protein level of NF-κB p65 in $AlCl_3$ group was higher ($p < 0.01$) than that in control group, and nuclear protein level of NF-κB p65 in the $AlCl_3$ + LYC group was lower than that in the $AlCl_3$ group ($p < 0.01$). The cytosolic protein level of NF-κB p65 in the $AlCl_3$ and the $AlCl_3$ + LYC group was lower ($p < 0.01$) than that in the control group, but the cytosolic protein level of NF-κB p65 in the $AlCl_3$ + LYC group was not different from that in the $AlCl_3$ group ($p > 0.05$).

3.7. Effects of LYC on Nrf2 and its downstream genes in the hippocampus of $AlCl_3$-exposed rats

As shown in Fig. 6, the nuclear protein level of Nrf2 in the $AlCl_3$, $AlCl_3$ + LYC and LYC group was higher ($p < 0.05$) than that in the control group, and the nuclear protein level of Nrf2 in the $AlCl_3$ + LYC group was higher ($p < 0.01$) than that in $AlCl_3$ group. The cytosolic protein level of Nrf2 in the $AlCl_3$, $AlCl_3$ + LYC and LYC group was lower ($p < 0.01$) than that in the control group, and the cytosolic protein level of Nrf2 in the $AlCl_3$ + LYC group was not different from that in the $AlCl_3$ group ($p > 0.05$). Additionally, the mRNA levels of HO-1, NQO1, GCLC and SOD1 in the $AlCl_3$, $AlCl_3$ + LYC and LYC group were higher than these in the control group ($p < 0.05$), and the mRNA levels of HO-1, NQO1, GCLC and SOD1 were in the $AlCl_3$ + LYC group higher ($p < 0.01$) than these in the $AlCl_3$ group.

4. Discussion

In this study, several important observations were obtained. First, LYC attenuated $AlCl_3$-induced cognition impairment and histopathological changes of the hippocampus in rats. Then, LYC reduced oxidative stress, apoptosis and inflammation in the hippocampus of $AlCl_3$-exposed rat. Finally, LYC increased nuclear translocation of Nrf2 and its downstream gene expression in the hippocampus of $AlCl_3$-exposed rats, indicating that activation of Nrf2 was involved in the protective effect of LYC against $AlCl_3$-induced hippocampal lesions.

Oxidative stress has been implicated with pathogenesis of

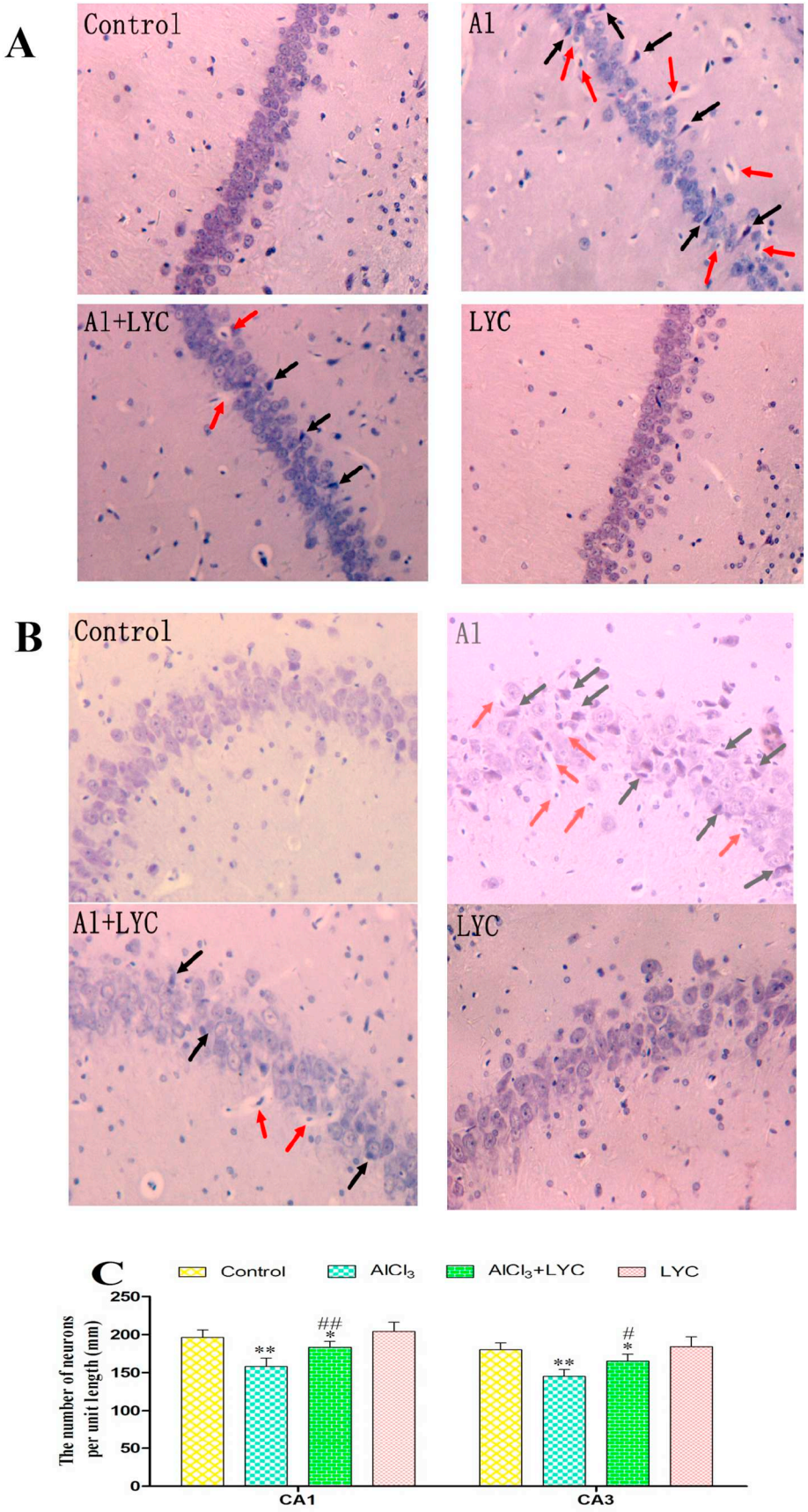

Fig. 3. Representative photomicrographs of The hippocampal histology (HE, magnification: 400×). (A) The hippocampal CA1 regions. (B) The hippocampal CA3 regions. (C) The number of neurons per unit length (mm) in hippocampus. The black arrow indicates necrosis and pyknotic nuclei. The red arrow indicates vacuolar spaces around cell cytoplasm. (For interpretation of the references to colour in this figure legend, the reader is referred to the web version of this article.)

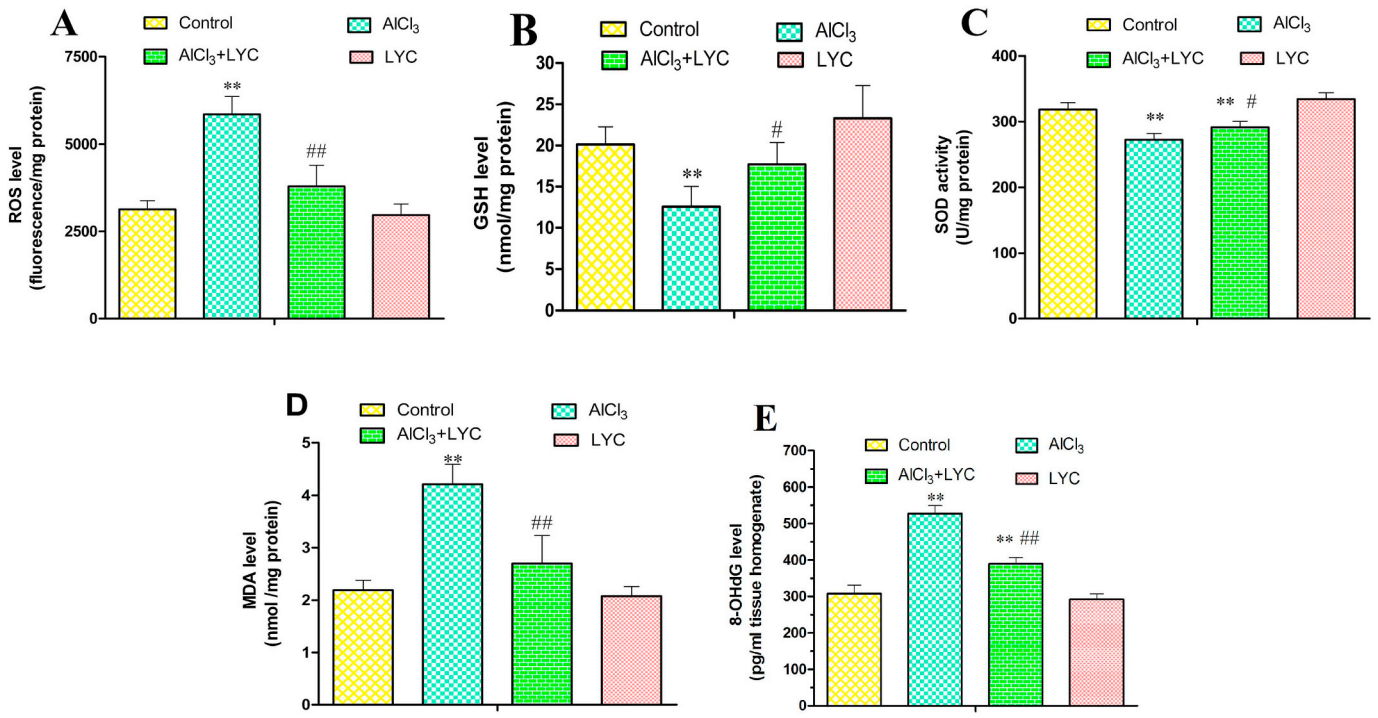

Fig. 4. Effects of LYC on oxidative stress in the hippocampus of $AlCl_3$-exposed rats.

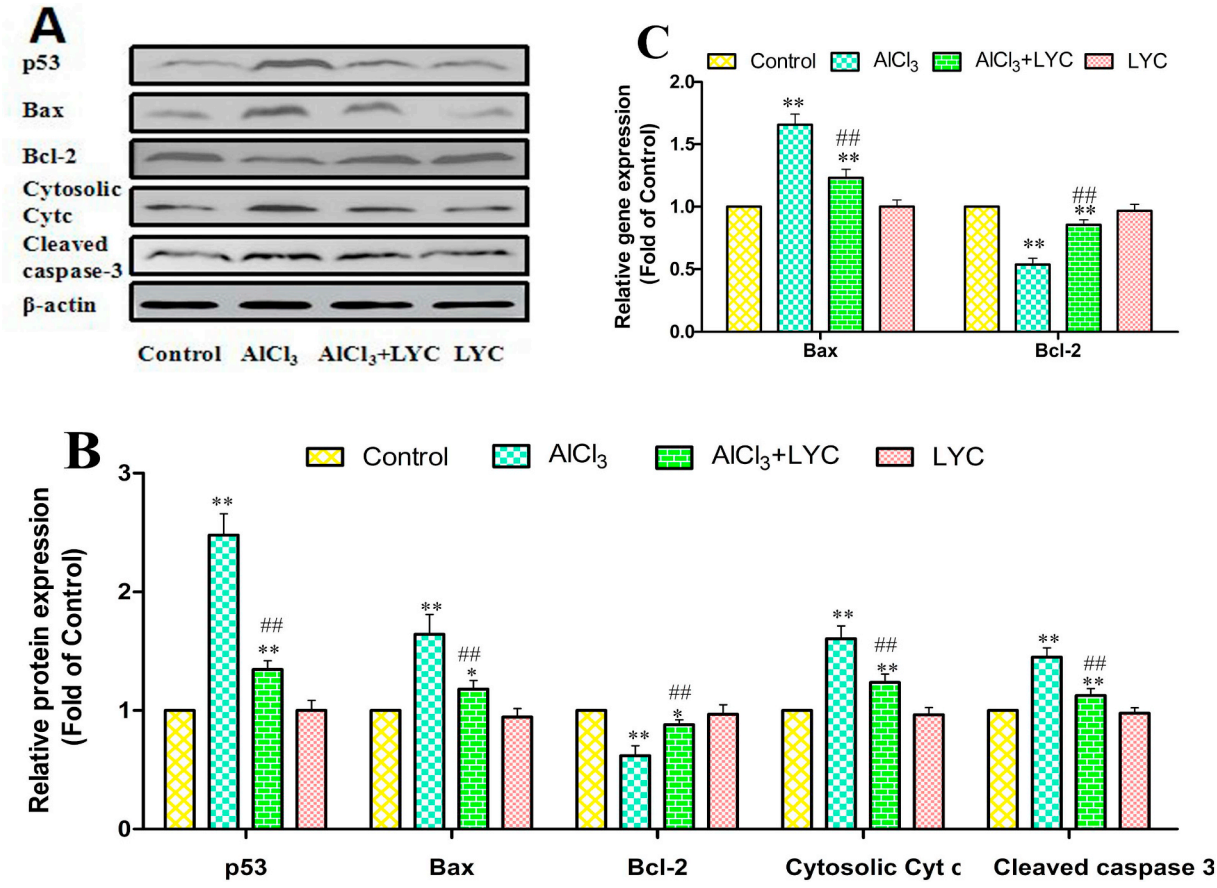

Fig. 5. (A) The p53, Bax, Bal-2, Cytosolic Cyt c and Cleaved caspase-3 protein expressions were assessed by Western blot. (B) The relative protein expressions of p53, Bax, Bal-2, Cytosolic Cyt c and Cleaved caspase-3. (C) The relative gene expressions of Bax and Bcl-2.

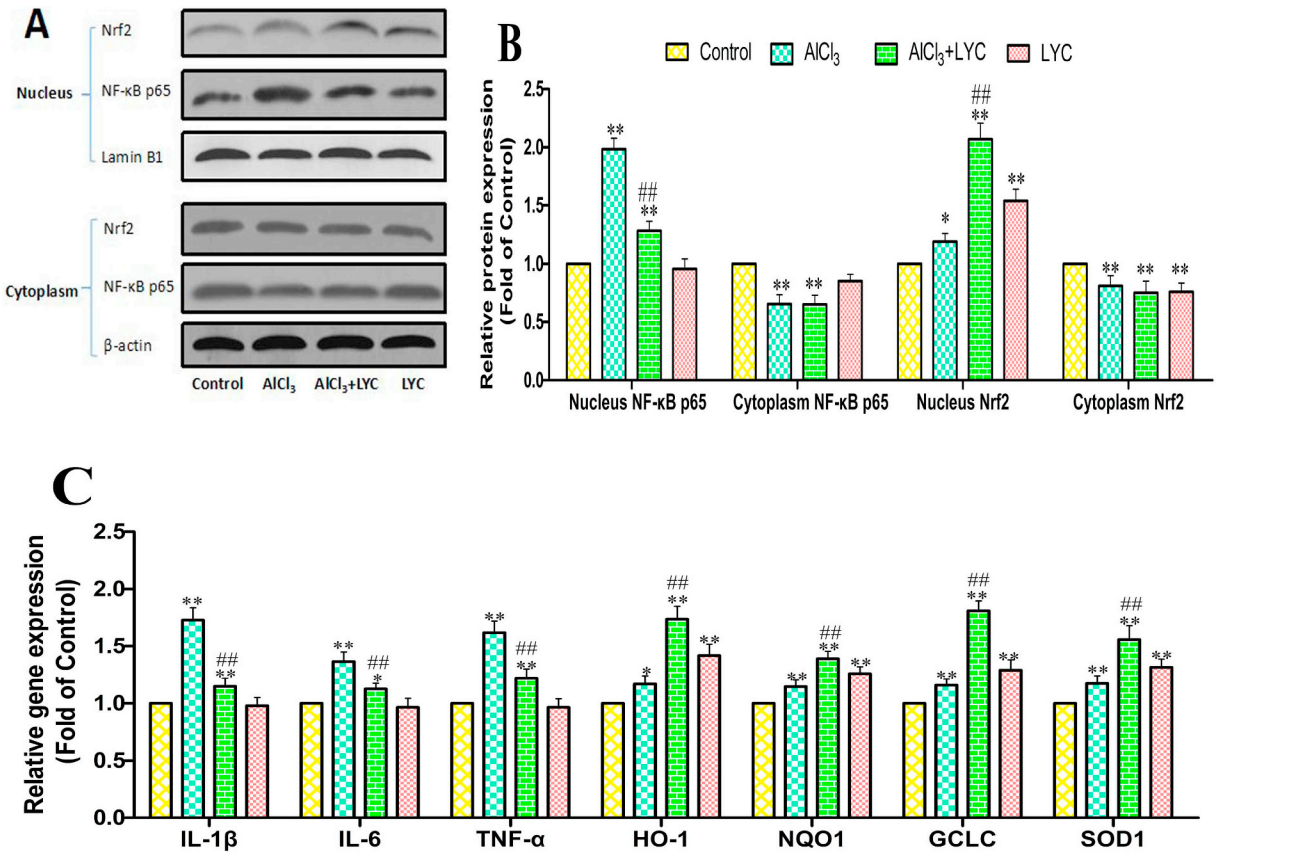

Fig. 6. (A) The NF-κB p65 and Nrf2 protein expressions were assessed by Western blot. (B) The relative protein expressions of NF-κB p65 and Nrf2. (C) The relative gene expressions of NF-κB p65 downstream pro-inflammatory cytokines and Nrf2 downstream target genes.

neurodegeneration [30], which is also widely accepted as the primary pathogenesis of Al neurotoxicity [11]. Our present study showed that LYC significantly reduced ROS, lipid peroxidation production MDA and DNA damage biomarker 8-OHdG level as well as elevated antioxidant enzyme SOD activity and GSH level in hippocampus of $AlCl_3$-exposed rats, indicating LYC protects hippocampus against $AlCl_3$-induced oxidative stress and peroxidation damage. Consistent with measurements of hippocampal-dependent learning and memory ability and the histological observations of hippocampus, LYC significantly attenuated $AlCl_3$-induced hippocampal lesions. Therefore, the mechanism underlying the protective effect of LYC against $AlCl_3$-induced hippocampal lesions may be the inhibition of oxidative stress.

Beyond exerting a direct toxic effect on biological macromolecules, oxidative stress induces neuropathological alterations including neuronal apoptosis and neuroinflammation, which are involved in the Al-induced hippocampal lesions [27,31]. Al has been reported to induce hippocampal nerve apoptosis via p53-dependent apoptotic pathway [10,31–33]. The p53, an important activator of the intrinsic apoptotic pathway, can be activated by DNA damage [34]. The activation of p53 has been shown to decrease anti-apoptotic member Bcl-2 and increase pro-apoptotic member Bax gene expression [35,36]. The imbalance between Bax and Bcl-2 induces mitochondrial membrane permeabilisation, and then causes the release of Cyt c from the mitochondria to activate the caspase cascade [37]. The activation of caspase-3 is the final executioner enzyme of apoptosis [38,39]. In present study, we found that administration of LYC significantly increased Bcl-2 level and decreased p53, Bax, cytoplasmic Cyt c and cleaved caspase-3 level in relative to the $AlCl_3$-treatment rats. These results suggested that LYC attenuated $AlCl_3$-induced hippocampal lesions, which is related to the suppression of ROS-induced p53-dependent apoptosis in rat. In addition, our present study showed that $AlCl_3$ increased p53 expression in the hippocampus as compared to control rats. The result is same as previous studies, which proved Al induce neuronal apoptosis via increasing p53 expression in the Neuro-2a cells and rodent hippocampus [31–33]. However, other research observed the opposite result. Mustafa Rizvi et al. study showed Al suppressed p53 expression and induced apoptosis via p53-independent apoptotic pathway in SH-SY5Y human neuroblastoma cells [17]. One possible cause is the species differences. Another possibility is the differences of experimental factor between the hippocampus in vivo and cell lines in vitro. Moreover, the neuroinflammation also is a mechanism of Al-induced hippocampal lesions [2,27]. NF-κB plays a critical role in the activation of neuroinflammatory pathway which causes transcriptions of pro-inflammatory mediators such IL-1β, IL-6 and TNF-α [40]. Our previous study indicated that NF-κB-mediated neuroinflammation occurred in $AlCl_3$-induced hippocampal lesions of rat [27]. However, LYC protects the hippocampus against neuroinflammation as evidenced by the fact that LYC inhibited the translocation of NF-κB p65 into the nucleus and the expression of proinflammatory cytokines in the present study. It is also noteworthy that neuroinflammation may be a consequence of chronic oxidative stress due to ROS-mediated NF-κB activation [15]. Taken together, all these results indicated that LYC attenuated $AlCl_3$-induced apoptosis and neuroinflammation in the hippocampus, and a possible explanation is that LYC protects the hippocampus against apoptosis and neuroinflammation via scavenging ROS.

To further explore the mechanisms underlying the protective effects of LYC on $AlCl_3$-induced hippocampal lesions, our study focused on Nrf2, as it shows antioxidant property by enhancing transcription of phase II detoxifying enzymes and antioxidant enzymes [16,40]. Surprisingly, we found $AlCl_3$ group exhibited a higher nucleus translocation of Nrf2 as well as mRNA levels of GCLC and SOD1 when compared to the control group, suggesting $AlCl_3$ could elevate Nrf2 activity to

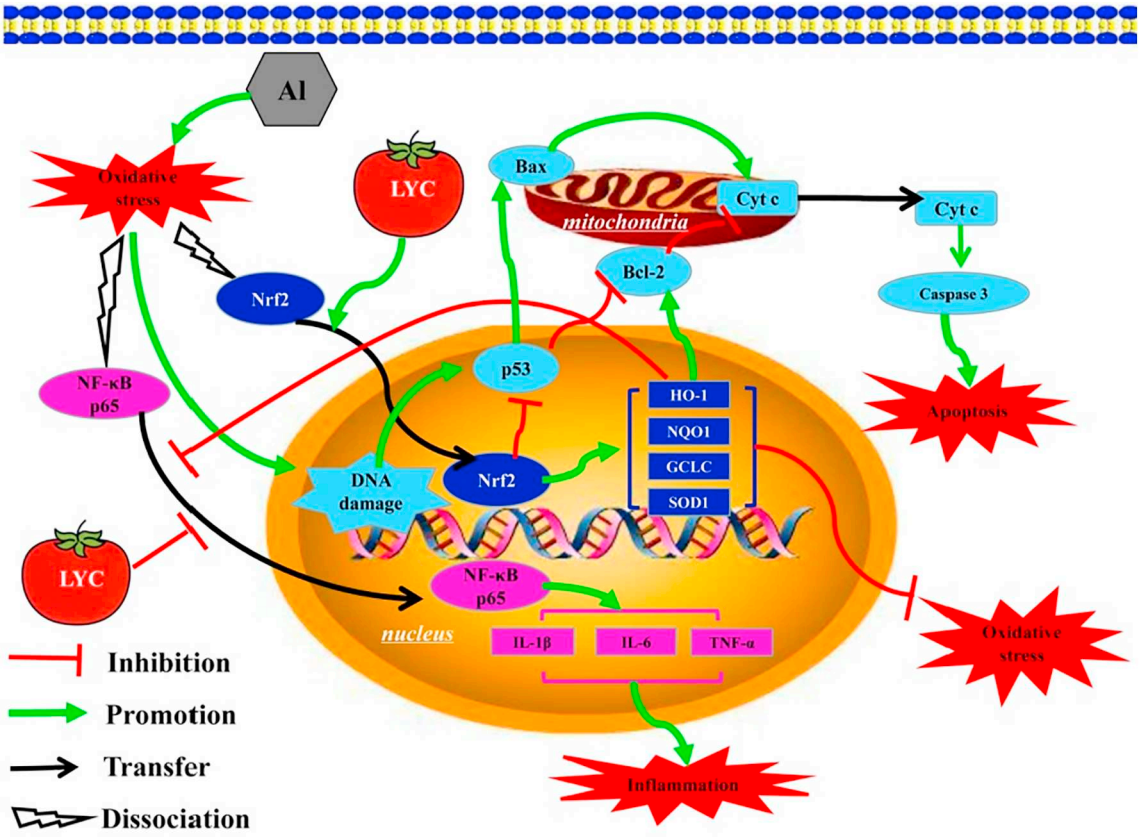

Fig. 7. LYC attenuates Al-induced hippocampal lesions by inhibiting oxidative stress-mediated inflammation and apoptosis in the rat.

enhance antioxidant defense system. It is well known that the enhanced production of free radicals can incite the translocation and the accrual of Nrf2 in the nucleus, and then increase the transcription of antioxidant proteins to enhance antioxidant defense system [41,42]. Thus, the above results maybe owing to the effect of ROS provoked by $AlCl_3$ on Nrf2. However, it is contrary to our initial results that $AlCl_3$ reduce SOD activity and GSH level. A possible explanation is the generation of free radicals provoked by $AlCl_3$ induces SOD and GSH depletion. In addition, many studies showed that exposure to pro-oxidants or pathological condition either increased or decreased the expression/activation of Nrf2 depending on the stage of disease and method of pro-oxidants administration [43,44]. Mustafa Rizvi et al. found 100 μM of $Al(mal)_3$ treatment increased Nrf2 level, and the concentrations within the range of 400 μM to 600 μM of $Al(mal)_3$ decreased Nrf2 level in SH-SY5Y neuroblastoma cells, indicating the effect of Al on the Nrf2 signal also depended on the concentration of Al [17]. Thus, the role of Nrf2 in $AlCl_3$-induced cognition impairment needs to be further clarified. Even so, our present study showed $AlCl_3$ + LYC group exhibited a higher nucleus translocation of Nrf2 as well as mRNA levels of HO-1, NQO1, GCLC and SOD1 when compared to $AlCl_3$ group. These results indicated that LYC increased Nrf2 nuclear translocation and its downstream genes to enhance antioxidant defense systems, thus efficiently neutralizing ROS during $AlCl_3$-induced neurotoxicity. Furthermore, some studies showed that p53 was negatively regulated by Nrf2, and HO-1 could upregulate expression of Bcl-2 and inhibited nuclear translocation of NF-κB [45–47]. Thus, activation of Nrf2 maybe the antioxidant mechanism of LYC, and partly contribute to explaining the inactivation of NF-κB p65 and p53 induced by LYC in the hippocampus of $AlCl_3$-exposed rat.

5. Conclusion

In summary, our findings reveal that LYC attenuates Al-induced hippocampal lesions by inhibiting oxidative stress-mediated inflammation and apoptosis in the rat (Fig. 7). Therefore, the use of LYC as a phytochemical supplement should be encouraged to prevent Al-induce hippocampal lesions.

Abbreviations

Al	Aluminum
$AlCl_3$	Aluminum chloride
Bax	Bcl-2-associated X protein
Bcl-2	B-cell lymphoma gene 2
Cyt c	Cytochrome c
GSH	Glutathione
HE	Hematoxylin and eosin
IL-6	Interleukin-6
IL-1β	Interleukin-1β
LYC	Lycopene
MDA	Malondialdehyde
MWM	Morris water maze
Nrf2	Nuclear factor-erythroid-2-related factor 2
NF-κB	Nuclear factor kappa B
ROS	Reactive oxygen species
SOD	Superoxide dismutase
TNF-α	Tumor necrosis factor α
8-OHdG	8-hydroxy-2′-deoxyguanosine

Supplementary data to this article can be found online at https://doi.org/10.1016/j.jinorgbio.2019.01.017.

Conflict of interest

The authors have no conflicts of interest to declare.

Acknowledgments

This work was supported by the National Natural Science Foundation Project (31872530), the National Key R&D Program of China (2017YFD0502200), the Earmarked Fund for China Agriculture Research System (CARS-35), and the Open Project Program of Northeastern Science Inspection Station, China Ministry of Agriculture Key Laboratory of Animal Pathogen Biology (DY201709).

References

[1] N.H. Zawilla, F.M. Taha, N.A. Kishk, S.A. Farahat, M. Farghaly, M. Hussein, Occupational exposure to aluminum and its amyloidogenic link with cognitive functions, J. Inorg. Biochem. 139 (2014) 57–64.
[2] C. Zheng, Y. Xu, H. Zhang, H. Wang, W. Huang, F. Xu, C. Zhuang, X. Wang, Y. Li, Aluminum chloride induces neuroinflammation, loss of neuronal dendritic spine and cognition impairment in developing rat, Chemosphere 151 (2016) 289–295.
[3] C.C. Willhite, G.L. Ball, C.J. McLellan, Total allowable concentrations of monomeric inorganic aluminum and hydrated aluminum silicates in drinking water, Crit. Rev. Toxicol. 42 (2012) 358–442.
[4] C.C. Willhite, N.A. Karyakina, R.A. Yokel, N. Yenugadhati, T.M. Wisniewski, I.M. Arnold, F. Momoli, D. Krewski, Systematic review of potential health risks posed by pharmaceutical, occupational and consumer exposures to metallic and nanoscale aluminum, aluminum oxides, aluminum hydroxide and its soluble salts, Crit. Rev. Toxicol. 44 (2014) 1–80.
[5] S.M. Saiyed, R.A. Yokel, Aluminium content of some foods and food products in the USA, with aluminium food additives, Food Addit. Contam. 22 (2005) 234–244.
[6] R.W. Smith, Kinetic aspects of aqueous aluminum chemistry: environmental implications, Coord. Chem. Rev. 149 (1996) 81–93.
[7] U. Borgmann, Y. Couillard, L.C. Grapentine, Relative contribution of food and water to 27 metals and metalloids accumulated by caged *Hyalella azteca* in two rivers affected by metal mining, Environ. Pollut. 145 (2007) 753–765.
[8] A. Kaur, K. Joshi, R.W. Minz, K.D. Gill, Neurofilament phosphorylation and disruption: a possible mechanism of chronic aluminium toxicity in Wistar rats, Toxicology 219 (2006) 1–10.
[9] S.M. Farhat, A. Mahboob, G. Iqbal, T. Ahmed, Aluminum-induced cholinergic deficits in different brain parts and its implications on sociability and cognitive functions in mouse, Biol. Trace Elem. Res. 177 (2016) 1–7.
[10] D.R. Sharma, A. Sunkaria, D. Verma, K.D. Gill, Quercetin attenuates aluminum-induced apoptosis in rat Hippocampus, by preventing cytochrome c translocation, Bcl-2 decrease, Bax elevation, Caspase-3 and p53 activation, Free Radic. Biol. Med. 53 (2012) S44–S45.
[11] V. Kumar, K.D. Gill, Oxidative stress and mitochondrial dysfunction in aluminium neurotoxicity and its amelioration: a review, Neurotoxicology 41 (2014) 154–166.
[12] H. Lu, J. Hu, J. Li, W. Pang, Y. Hu, H. Yang, W. Li, C. Huang, M. Zhang, Y. Jiang, Optimal dose of zinc supplementation for preventing aluminum-induced neurotoxicity in rats, Neural Regen. Res. 8 (2013) 2754–2762.
[13] J.A. Smith, A. Das, S.K. Ray, N.L. Banik, Role of pro-inflammatory cytokines released from microglia in neurodegenerative diseases, Brain Res. Bull. 87 (2012) 10–20.
[14] R.V. Bernhardi, L.E. Bernhardi, J. Eugenín, Microglial cell dysregulation in brain aging and neurodegeneration, Front. Aging Neurosci. 7 (2015) 124.
[15] J.M. Taylor, B.S. Main, P.J. Crack, Neuroinflammation and oxidative stress: co-conspirators in the pathology of Parkinson's disease, Neurochem. Int. 62 (2013) 803–819.
[16] I. Buendia, P. Michalska, E. Navarro, I. Gameiro, J. Egea, R. León, Nrf2-ARE pathway: an emerging target against oxidative stress and neuroinflammation in neurodegenerative diseases, Pharmacol. Ther. 157 (2016) 84–104.
[17] S.H. Mustafa Rizvi, A. Parveen, A.K. Verma, I. Ahmad, M. Arshad, A.A. Mahdi, Aluminium induced endoplasmic reticulum stress mediated cell death in SH-SY5Y neuroblastoma cell line is independent of p53, PLoS One 9 (2014) e98409.
[18] R. Zhang, J. Zhang, L. Fang, X. Li, Y. Zhao, W. Shi, A. Li, Neuroprotective effects of Sulforaphane on cholinergic neurons in mice with Alzheimer's disease-like lesions, Int. J. Mol. Sci. 15 (2014) 14396.
[19] J. Pirayesh Islamian, H. Mehrali, Lycopene as a carotenoid provides radioprotectant and antioxidant effects by quenching radiation-induced free radical singlet oxygen: an overview, Cell J. 16 (2015) 386–391.
[20] W. Mellert, K. Deckardt, C. Gembardt, S. Schulte, R.B. Van, R. Slesinski, Thirteen-week oral toxicity study of synthetic lycopene products in rats, Food Chem. Toxicol. 40 (2002) 1581–1588.
[21] I.M. Petyaev, Lycopene deficiency in ageing and cardiovascular disease, Oxidative Med. Cell. Longev. 2016 (2016) 3218605.
[22] S.K. Clinton, Lycopene: chemistry, Biology, and implications for human health and disease, Nutr. Rev. 56 (2010) 35–51.
[23] S. Hwang, J.W. Lim, H. Kim, Inhibitory Effect of Lycopene on Amyloid-β-Induced Apoptosis in Neuronal Cells, Nutrients 9 (2017) 883.
[24] J. Wang, L. Li, Z. Wang, Y. Cui, X. Tan, T. Yuan, Q. Liu, Z. Liu, X. Liu, Supplementation of lycopene attenuates lipopolysaccharide-induced amyloidogenesis and cognitive impairments via mediating neuroinflammation and oxidative stress, J. Nutr. Biochem. 56 (2018) 16–25.
[25] B. Zhao, B. Ren, R. Guo, W. Zhang, S. Ma, Y. Yao, T. Yuan, Z. Liu, X. Liu, Supplementation of lycopene attenuates oxidative stress induced neuroinflammation and cognitive impairment via Nrf2/NF-κB transcriptional pathway, Food Chem. Toxicol. (2017) 505–516.
[26] Q. Yin, Y. Ma, Y. Hong, X. Hou, J. Chen, C. Shen, M. Sun, Y. Shang, S. Dong, Z. Zeng, Lycopene attenuates insulin signaling deficits, oxidative stress, neuroinflammation, and cognitive impairment in fructose-drinking insulin resistant rats, Neuropharmacology 86 (2014) 389–396.
[27] H. Zhang, P. Wang, H. Yu, K. Yu, Z. Cao, F. Xu, X. Yang, M. Song, Y. Li, Aluminum trichloride-induced hippocampal inflammatory lesions are associated with IL-1β-activated IL-1 signaling pathway in developing rats, Chemosphere 203 (2018) 170–178.
[28] M. Sun, S. Chen, Determination of trace amounts of aluminum in rat brain by GFAAS, Phys. Test. Chem. Anal., Part B 43 (2007) 1070–1072.
[29] F. Xu, Y. Liu, H. Zhao, K. Yu, M. Song, Y. Zhu, Y. Li, Aluminum chloride caused liver dysfunction and mitochondrial energy metabolism disorder in rat, J. Inorg. Biochem. 174 (2017) 55–62.
[30] S. Salim, Oxidative stress and the central nervous system, J. Pharmacol. Exp. Ther. 360 (2016) 201–205.
[31] D.R. Sharma, W.Y. Wani, A. Sunkaria, R.J. Kandimalla, R.K. Sharma, D. Verma, A. Bal, K.D. Gill, Quercetin attenuates neuronal death against aluminium induced neurodegeneration in the rat hippocampus, Neuroscience 324 (2016) 163–176.
[32] P. Dharmalingam, G. Sudhandiran, Dietary flavonoid fisetin regulates aluminium chloride-induced neuronal apoptosis in cortex and hippocampus of mice brain, J. Nutr. Biochem. 26 (2015) 1527–1539.
[33] V.J. Johnson, S.H. Kim, R.P. Sharma, Aluminum-maltolate induces apoptosis and necrosis in neuro-2a cells: potential role for p53 signaling, Toxicol. Sci. 83 (2005) 329–339.
[34] K.E. Gurley, R. Moser, Y. Gu, P. Hasty, C.J. Kemp, DNA-PK suppresses a p53-independent apoptotic response to DNA damage, EMBO Rep. 10 (2009) 87–93.
[35] T. Miyashita, J.C. Reed, Tumor suppressor p53 is a direct transcriptional activator of the human bax gene, Cell 80 (1995) 293–299.
[36] T. Miyashita, M. Harigai, M. Hanada, J.C. Reed, Identification of a p53-dependent negative response element in the bcl-2 gene, Cancer Res. 54 (1994) 3131–3135.
[37] B. Antonsson, Mitochondria and the Bcl-2 family proteins in apoptosis signaling pathways, Mol. Cell. Biochem. 256–257 (2004) 141–155.
[38] S. Mazumder, D. Plesca, A. Almasan, Caspase-3 activation is a critical determinant of genotoxic stress-induced apoptosis, Methods Mol. Biol. 414 (2008) 13–21.
[39] M.A. Savitskaya, G.E. Onishchenko, Mechanisms of apoptosis, Biochemistry 80 (2015) 1393–1405.
[40] T. Shabab, R. Khanabdali, S.Z. Moghadamtousi, H.A. Kadir, G. Mohan, Neuroinflammation pathways: a general review, Int. J. Neurosci. 127 (2016) 624–633.
[41] K. Itoh, K.I. Tong, M. Yamamoto, Molecular mechanism activating Nrf2-Keap1 pathway in regulation of adaptive response to electrophiles, Free Radic. Biol. Med. 36 (2004) 1208–1213.
[42] H.E. de Vries, M. Witte, D. Hondius, A.J. Rozemuller, B. Drukarch, J. Hoozemans, H.J. Van, Nrf2-induced antioxidant protection: a promising target to counteract ROS-mediated damage in neurodegenerative disease? Free Radic. Biol. Med. 45 (2008) 1375–1383.
[43] Y. Zou, R. Wang, H. Guo, M. Dong, Phytoestrogen β-ecdysterone protects PC12 cells against MPP + -induced neurotoxicity in vitro: involvement of PI3K-Nrf2-regulated pathway, Toxicol. Sci. 147 (2015) 28–38.
[44] M. Mcmahon, K. Itoh, M. Yamamoto, J.D. Hayes, Keap1-dependent proteasomal degradation of transcription factor Nrf2 contributes to the negative regulation of antioxidant response element-driven gene expression, J. Biol. Chem. 278 (2003) 21592–21600.
[45] B. Ke, X.D. Shen, F. Gao, B. Qiao, H. Ji, R.W. Busuttil, H.D. Volk, J.W. Kupiec-Weglinski, Small interfering RNA targeting heme oxygenase-1 (HO-1) reinforces liver apoptosis induced by ischemia-reperfusion injury in mice: HO-1 is necessary for cytoprotection, Hum. Gene Ther. 20 (2009) 1133–1142.
[46] C. Lu, W. Xu, F. Zhang, J. Shao, S. Zheng, Nrf2 knockdown disrupts the protective effect of curcumin on alcohol-induced hepatocyte necroptosis, Mol. Pharm. 13 (2016) 4043–4053.
[47] D.S. Lee, K.S. Kim, W. Ko, B. Li, S. Keo, G.S. Jeong, H. Oh, Y.C. Kim, The neoflavonoid latifolin isolated from MeOH extract of *Dalbergia odorifera* attenuates inflammatory responses by inhibiting NF-κB activation via Nrf2-mediated heme oxygenase-1 expression, Phytother. Res. 28 (2014) 1216–1223.